13th World Conference on Earthquake Engineering
Vancouver, B.C., Canada
August 1-6, 2004
Paper No. 1403

EXPERIMENTS ON SHEAR-FLEXURAL BEHAVIORS OF MODEL CAST IN PLACE CONCRETE PILES

Toshihiko YAMAMOTO[1]
Kazuo YAMADA[2]
Akira OKADA[3]

SUMMARY

An experimental investigation was performed to examine the shear-flexural behaviors of cast in place concrete piles with nineteen model specimens. The specimens had a 300mm or 400mm circular section with stubs at both ends and the shear-span ratios (M/QD) were either 1.5 or 2.0. The variables of the experiments were M/QD, shear reinforcing ratio, strength grades of shear reinforcement and axial stress levels. Since there are no reliable equations for estimating the shear strength of cast in place concrete piles, the Ohno-Arakawa equations for estimating ultimate shear strength of reinforced concrete rectangular section members were modified and used for the calculation. Although the average shear strength of the specimens was 1.2 to the calculated strength, each data was somewhat scattered. The minimum shear reinforcing ratios were necessary to ensure the flexural or ultimate flexural strength of the specimens respectively. The deformational characteristics varied with the shear reinforcing ratios. It is needed to develop an equation for estimating the shear strength of concrete piles directly in conjunction with their deformation.

INTRODUCTION

Recently considerable structural damages of substructures caused by severe earthquakes have been reported [1]. Therefore, it is necessary to research their seismic performance in a hurry. Concerning cast in place concrete piles, there is little information on their seismic behaviors [2-4]. Because the flexural and shear reinforcing ratios of such piles are quite low compared with super structures, the conventional equations are not adequate to this type of piles. An experimental investigation was performed to examine the shear-flexural behaviors of cast in place concrete piles with nineteen model specimens.
The variables of this test were M/QD, shear reinforcing ratio, strength grades of shear reinforcement and axial stress levels. The M/QD 1.5 and 2.0 were selected from the moment distributions along piles in soil at high shear stress regions. The shear reinforcing ratios 0.00%, 0.10% and 0.20% were also selected considering the current pile design practice and that of 0.30% was added for comparison. High strength shear reinforcing steels were used to examine their efficiency. It is important to provide sufficient space

[1] Daido Institute of Technology
[2] Aichi Institute of Technology
[3] Yokon Co., Ltd.

between lateral reinforcing bars for underground concreting. Including the cases of expanded bottom piles and stress changes in seismic action, the axial stress levels (N) were 0, 7.5, 15 MPa and variable (-2.5 to 7.5MPa),. Three series of experiments were performed to examine the effect of the variables above mentioned on the seismic performance of the specimens.
Since there is no reliable equation for estimating the shear strength of cast in place concrete piles, the Ohno-Arakawa equations for estimating ultimate shear strength of reinforced concrete rectangular section members were modified and used for the calculation. The specimens were designed to reach their shear strength before ultimate flexural strength. Because of the circular section the extreme tension longitudinal bars tend to yield in the early stage before reaching the ultimate flexural strength. Therefore the deformational characteristics were also examined in terms of lateral displacement.

OUTLINE OF EXPERIMENTS

Specimens

The specimens are shown in Fig.1 (Shear-Span Ratio *M/QD*=2.0) and listed in Table 1. The specimens had a 300mm or 400mm circular section with stubs at both ends and the shear-span ratios (*M/QD*) were either 1.5 or 2.0. The variables of the experiments were *M/QD*, shear reinforcing ratio, strength grades of lateral reinforcement and axial stress levels. The shear reinforcing ratios were 0.00%, 0.10%, 0.20% and 0.30%. Normal and high strength lateral reinforcing steels were used. The axial stress levels (N) were 0, 7.5, 15 MPa and variable (-2.5 to 7.5MPa). The longitudinal bars were 12-D16 or 20-D16 (p_g=3.37% or 3.17%, SD390, cover 30mm or 40mm).

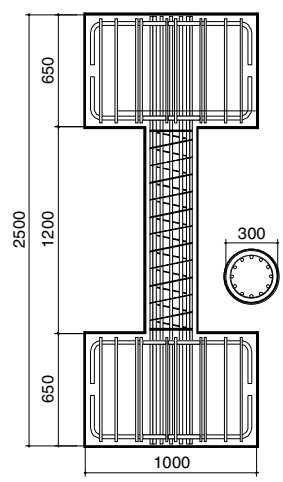

Fig.1 Specimen (*M*/*QD*=2.0)

Flexure and shear strength

The flexural ${}_cQ_{my}$ and ultimate flexural strength ${}_cQ_{mu}$ were calculated from the e function method [5]. The shear strength ${}_cQ_{su}$ was calculated from the modified Ohno-Arakawa equations (1) [6], converting the actual circular sections into equivalent rectangular sections. The tension longitudinal bars were assumed to be 1/4 of the gross longitudinal bars in the equation.

$$Q_u = \left\{ \frac{0.12 k_u \cdot k_p (180 + F_c)}{M/Qd + 0.12} + 2.7\sqrt{p_w \sigma_{wy}} + 0.1\sigma_o \right\} b \cdot j \qquad (1)$$

where Q_u =shear strength (kgf); k_u =coefficient of effective depth; $k_p = p_t{}^{0.23}$; F_c =concrete strength (kgf/cm^2); M/Qd =shear span ratio; p_w =lateral reinforcing ratio; σ_{wy} =yield point of lateral reinforcing steel (kgf/cm^2); σ_o =axial stress (kgf/cm^2); $d = 0.9 \times 0.89D$, $b = 0.89D$ (D :diameter, cm); $j = 7/8d$; $p_t = p_g/4$ (%).

Table 1 Specimens

Specimen	Diameter (mm)	Shear-span ratio M/QD	Bar arrangement: Longitudinal	*pg* (%)	Lateral	*pw* (%)	Axial stress *N* (MPa)	Calculated strength: Flexure# *cQmy* (kN)	Flexure# *cQmu* (kN)	Shear## *cQsu* (kN)	Experiment Series
No.1	300	1.50	12-D16	3.38	4φ@100*	0.095	7.5	244	282	172	II
No.2	〃	〃	〃	〃	4φ@50	0.189	0	163	228	152	I
No.3	〃	〃	〃	〃	〃	〃	〃	171	238	144	II
No.4	〃	〃	〃	〃	〃	〃	7.5	236	279	193	I
No.5	〃	〃	〃	〃	4φ@50*	〃	〃	244	282	185	II
No.6	〃	2.00	〃	〃	0	0	0	122	171	81.4	I
No.7	〃	〃	〃	〃	4φ@100	0.095	0	122	171	114	〃
No.8	〃	〃	〃	〃	〃	〃	7.5	177	209	154	〃
No.9	〃	〃	〃	〃	4φ@100**	〃	〃	183	212	170	II
No.10	〃	〃	〃	〃	4φ@100	〃	15	210	216	195	I
No.11	〃	〃	〃	〃	〃	〃	-2.5,7.5	205	208	149	II
No.12	〃	〃	〃	〃	4φ@50	0.189	0	122	171	127	I
No.13	〃	〃	〃	〃	〃	〃	7.5	177	209	168	〃
No.14	〃	〃	〃	〃	4φ@33	0.287	0	128	178	133	II
No.15	〃	〃	〃	〃	〃	〃	7.5	183	212	174	〃
No.16	400	1.50	20-D16	3.17	5φ@120**	0.092	7.5	415	475	304	III
No.17	〃	〃	〃	〃	5φ@60**	0.185	0	287	400	265	〃
No.18	〃	〃	〃	〃	〃	〃	7.5	415	475	337	〃
No.19	〃	〃	〃	〃	5φ@40**	0.277	〃	〃	〃	363	〃

* separate hoop, ** high strength hoop, # e function method, ## Ohno-Arakawa equation

Materials

The mix proportions and mechanical properties of the concrete are shown in Table 2. The concrete strength of the specimens was assumed to be the same as the test pieces taken at the time of casting and cured in the sealed condition. The strengths of the concrete were 29.5MPa, 26.1MPa and 25.5MPa at the experiments. The mechanical properties of steels are shown in Table 3. Main bars and spiral bars for lateral reinforcement were D16 and φ4, φ5, respectively. The separate hoops were made of the same $\phi 4$ bars for the spirals.

Table 2 Properties of concrete

Series	W/C (%)	Cement (kg/m^3)	Water (kg/m^3)	Slump (mm)	Tensile strength (MPa)	Compressive strength (MPa)	Young's modulus (GPa)
I	61.2	292	178	180	2.36	29.5	21.3
II	〃	〃	〃	〃	2.14	26.1	23.5
III	〃	〃	〃	〃	—	25.5	26.1

Table 3 Properties of reinforcing steel

Use	Series	Bar type & diameter	Yield point (MPa)	Tensile strength (MPa)	Young's modulus (GPa)
Longitudinal	I	D16	415	585	218
	II	〃	449	667	193
	III	〃	446	609	206
Lateral	I	φ4	494	562	207
	II	〃	502	624	203
	〃	φ4*	1420	1730	209
	III	φ5*	993	1280	204

D: deformed bar, φ: plain bar, * high strength

Test procedures

The loading and measuring systems are shown in Fig.2. The lateral load was applied to the specimens under a control of relative displacement angles (*R*) between two end stubs: single cycle at *R*=1/400rad, two cycles at *R*=1/200rad, 1/100rad and 1/50rad, single cycle at 1/25rad and monotonically loaded to 1/20rad as a general rule. Wire strain gauges were put on the four side of the longitudinal bars at five (*M/QD*=2.0) or four (*M/QD*=1.5) points; three or two points 1/2D in the test span and two in the stubs. Wire strain gauges were also put on lateral reinforcement at four points (1/2D and D from the stub). The zero initial readings of the strains were made after axial stress loading with no lateral load.

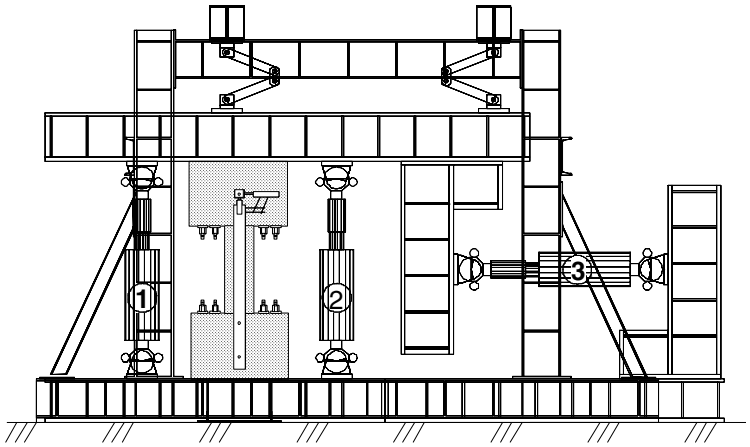

Fig. 2 Loading system (①,②:axial load, ③:lateral shear load)

RESULTS OF EXPERIMENTS

Progress of experiments and cracking

The results of experiments are shown in Table 4. The typical crack patterns of the specimens at the maximum strength are shown in Fig. 3. In every specimen flexural cracks occurred at first and then flexural-shear cracks occurred. In shear-span ratio *M/QD*=1.5, many cracks were observed in axially loaded No.4 specimen compared with non-axially loaded No.2 specimen. In *M/QD* 2.0, many extended cracks were also observed in 7.5MPa axially loaded specimens compared with non-axially loaded specimens. However, the number of shear cracks was not so many in 15MPa axially loaded No.10

Table 4 Results of experiments

Specimen	Shear-span ratio	Lateral reinforce	Axial stress	Maximum strength		0.8e*Q*	Failure	Ratio		
				e*Q*	eδ	δ 1 im	mode	Flexural		Shear
	M/*QD*	*pw*	*N*		$\times 10^{-3}$	$\times 10^{-3}$		*eQ*/*cQmy*	*eQ*/*cQmu*	*eQ*/*cQsu*
		(%)	(MPa)	(KN)	(rad)	(rad)				
No.1	1.50	0.095	7.5	200	4.98	-	S	0.82	0.71	1.16
No.2	〃	0.189	0	172	10.5	-	F1,S	1.06	0.75	1.13
No.3	〃	〃	〃	180	10.0	17.0	F1,S	1.05	0.76	1.25
No.4	〃	〃	7.5	256	10.2	11.8	F1,S	1.08	0.92	1.33
No.5	〃	〃	〃	234	8.38	20.0	F1,S	0.96	0.83	1.26
No.6	2.00	0	0	114	8.73	9.86	S	0.93	0.67	1.40
No.7	〃	0.095	0	119	7.85	8.68	S	0.98	0.70	1.04
No.8	〃	〃	7.5	188	10.1	11.4	F1,S	1.06	0.90	1.22
No.9	〃	〃	〃	196	10.0	20.0	F1,S	1.07	0.92	1.15
No.10	〃	〃	15	225	9.35	10.0	F2,S	1.07	1.04	1.15
No.11	〃	〃	-2.5,7.5	192	10.1	14.5	F1,S	0.94	0.92	1.29
No.12	〃	0.189	0	153	16.1	17.7	F1,S	1.25	0.89	1.20
No.13	〃	〃	7.5	205	14.3	20.4	F1,S	1.16	0.98	1.22
No.14	〃	0.287	0	194	40.2	40.2	F2	1.52	1.09	1.46
No.15	〃	〃	7.5	245	20.1	31.5	F2	1.34	1.16	1.41
No.16	1.50	0.092	7.5	344	5.00	10.0	S	0.83	0.72	1.13
No.17	〃	0.185	0	350	20.0	35.0	F1,S	1.22	0.88	1.32
No.18	〃	〃	7.5	409	10.0	36.0	F1,S	0.99	0.86	1.21
No.19	〃	0.277	〃	464	20.0	40.0	F2	1.12	0.98	1.28

specimen. From the viewpoint of the shear reinforcing ratios, many cracks were observed in 0.189% shear reinforced and non-axially loaded No.12 specimen compared with 0.095% reinforced No.7. On the contrary the number of cracks of 7.5MPa axially loaded specimen decreased as the shear reinforcing ratios increase. All the specimens except pw=0.27% reinforced specimens failed finally in shear.

Flexural and shear strength and failure mode

In the circular sections the extreme tension longitudinal bars tend to yield (*Qmy*) in the early stage of the experiments before reaching the ultimate flexural strength (*Qmu*) as shown in Fig. 4. Generally the calculation of the flexural strength is approximately accurate compared with that of the shear strength. Therefore it is possible to take these flexural strengths into consideration first for deciding the shear failure modes of the specimens. The failure modes of the specimens shown in Table 4 are divided into three patterns. They are shear failure (S), shear failure after flexural yielding (F1,S) and flexural or shear failure after ultimate flexural strength (F2). The lateral reinforcing ratios of the shear failure mode specimens are less than pw=0.10%. Those of the ultimate flexural mode specimens are more than pw=0.27%. Those of the shear failure after flexural yielding mode specimens are between the two ratios.

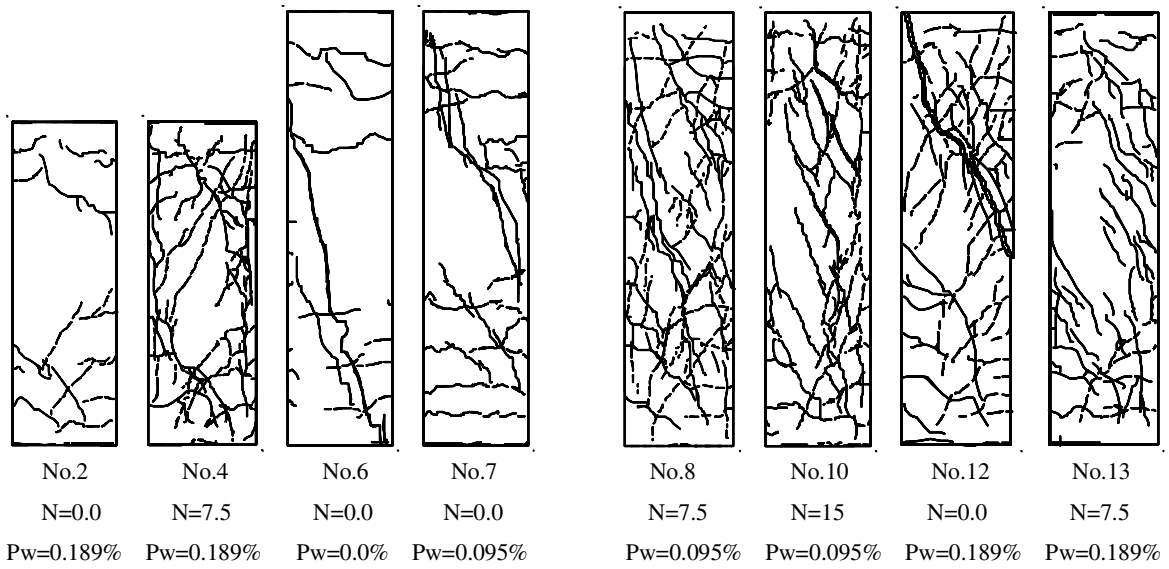

Fig. 3 Crack pattern at maximum strength

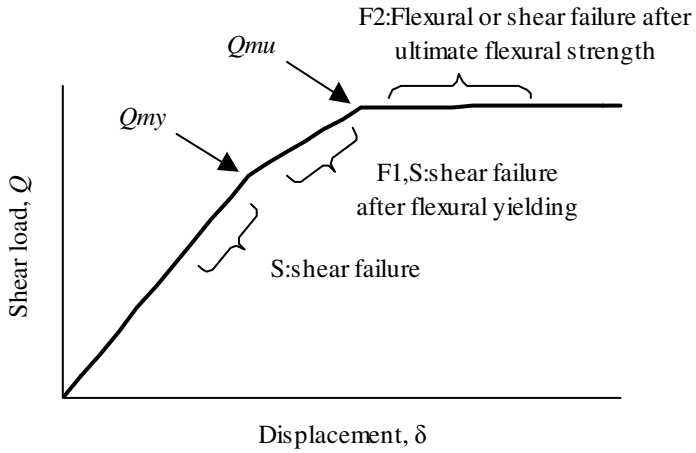

Fig. 4 Schematic load-displacement interaction and failure mode

Load-displacement relationship

The relationships between shear load and skeletons of the relative displacement are shown in Figs. 5 and 6. Fig.5 shows the difference of shear reinforcing ratios (M/QD=2.0: 0%, 0.095%, 0.189%, N=0). No.6 specimen failed in shear just after the shear cracking occurred. The shear stress at the failure was 1.61MPa and it was 1/18 and 1/1.5 of the compressive and tensile concrete strength, respectively. The shear strength of No.7 specimen, which had the shear reinforcing ratio of 0.095% ($p_w \cdot {}_w\sigma_y$ = 0.47MPa) was about the same and showed also a sudden decrease in strength. On the other hand, due to higher shear reinforcement ratio (0.189%), the displacement of No.12 specimen at the peak load was about twice as much as those of No.6 and No.7 specimens.

Fig. 6 shows the curves of the three specimens with the same shear reinforcement ratio of 0.095% tested

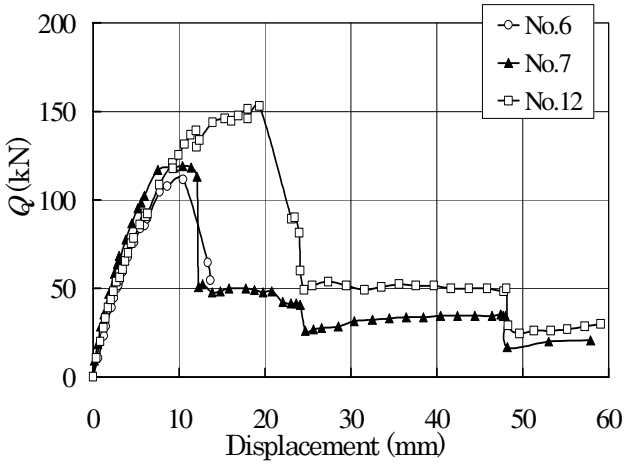

Fig.5 Load-displacement relationship (*M*/*QD*=2.0: *pw*=0%, 0.095%, 0.189%, *N*=0)

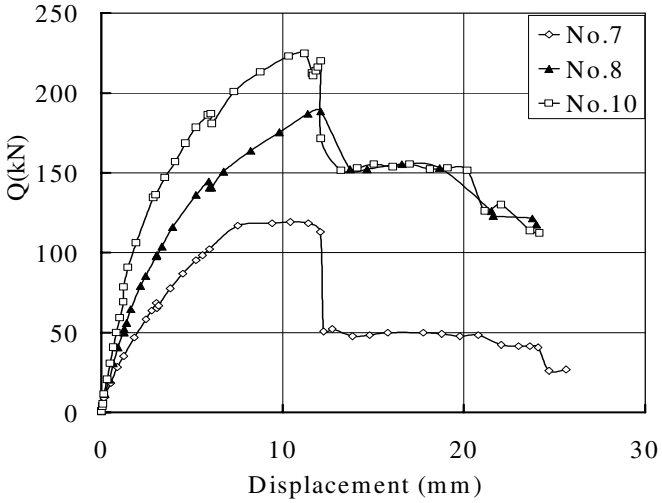

Fig.6 Load-displacement relationship (*M*/*QD*=2.0: *N*=0.0MPa, 7.5MPa , 15MPa, *pw*=0.095%)

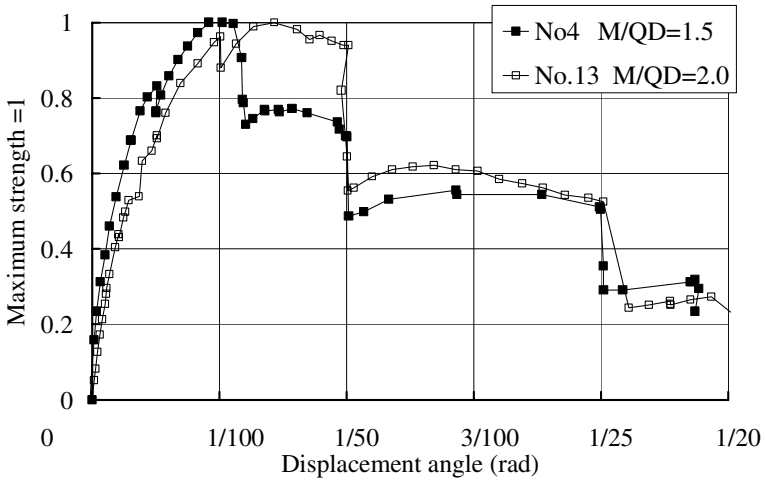

Fig. 7 Normalized load-displacement angle relationship (*pw*=0.189, *N*=7.5MPa)

under different axial loads. The axial stresses were 0.0MPa, 7.5MPa and 15MPa. Although the shear strengths differed so much, the displacement angles were about the same. Fig. 7 shows the normalized strength (maximum strength=1.0)-displacement angle relationships of No.4 and No.13 specimens. They had the same shear reinforcing ratio of 0.189% and axial stress of 7.5MPa. The shear-span ratios were 1.5 and 2.0 for No.4 and No.13 specimens, respectively. No.13 specimen showed stable behavior until relative displacement angle of 1/50 (rad) after reached the maximum strength. On the other hand No.4 specimen collapsed just after reached the maximum strength.

Lateral reinforcing ratio

The effects of lateral reinforcement ratios on the shear strength are shown in Fig.8 including high strength lateral reinforcement (H.S.). It is important to examine the effect of low lateral reinforcing ratios on the shear strength of concrete piles. Because in the current cast in place concrete pile design the shear reinforcing ratios are usually less than 0.20% ($p_w \cdot {}_w\sigma_y$ = 1.0MPa). Fig.8 shows that the shear strength increased in proportion to the lateral reinforcing ratio above 0.5 MPa.

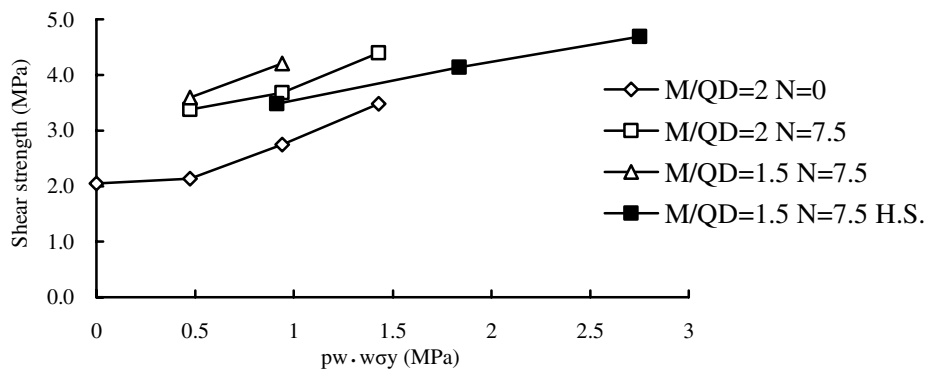

Fig. 8 Shear strength-lateral reinforcing ratio relationship

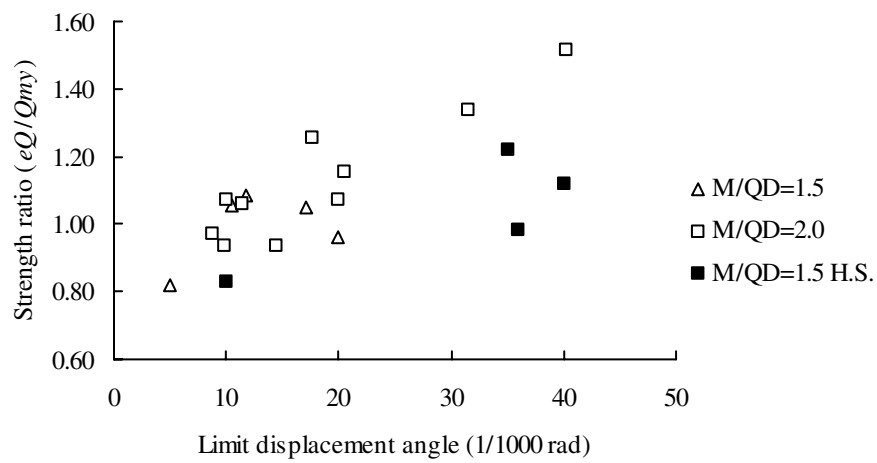

Fig. 9 Strength ratio-Limit displacement ralationship

Limit displacement

It is assumed that the limit displacement is the displacement at 0.8 of the maximum strength in descending part of the load-displacement skeletons. The relationship between strength ratio (*eQ*/*Qmy*) and limit displacement angle is shown in Fig. 9. The specimens exceeded the yield strength (*Qmy*) showed

large limit displacement angles. After yielding of the extreme tension longitudinal bars, the flexural displacements of the specimens become large. The specimens laterally reinforced over this strength confirmed the limit displacement angle of 1/00rad.
The relationship between strength ratio (*eQ*/*Qmu*) and limit displacement angle is shown in Fig. 10. The specimens exceeded the ultimate flexural strength (*Qmu*) except No.10 specimen (N=15MPa) showed large limit displacement angles. They were more than 3/100rad.

Comparison with calculated strength
The Ohno-Arakawa equation, AIJ:A method [7] and B method [7] are used for calculations. The maximum strengths of all the specimens exceeded the shear strength calculated from the three equations and methods. The comparisons between the test results and the calculations are shown in Table 5 and Fig. 11. Except No.14, No.15 and No.19 specimens (*pw*=0.287%, 0.277) all the specimens did not reach their ultimate flexural strength. Finding from the measured strain of the longitudinal bars, No.10 specimen also did not reach the ultimate flexural strength condition. The factors in the Ohno-Arakawa equations for calculating the shear strength are shear reinforcing and longitudinal reinforcing ratios, concrete strength, shear-span ratio, concrete depth and axial stress. The Ohno-Arakawa equations are relatively in good agreement with the experimental results. The average strength ratio to the Ohno-Arakawa equation was 1.24.

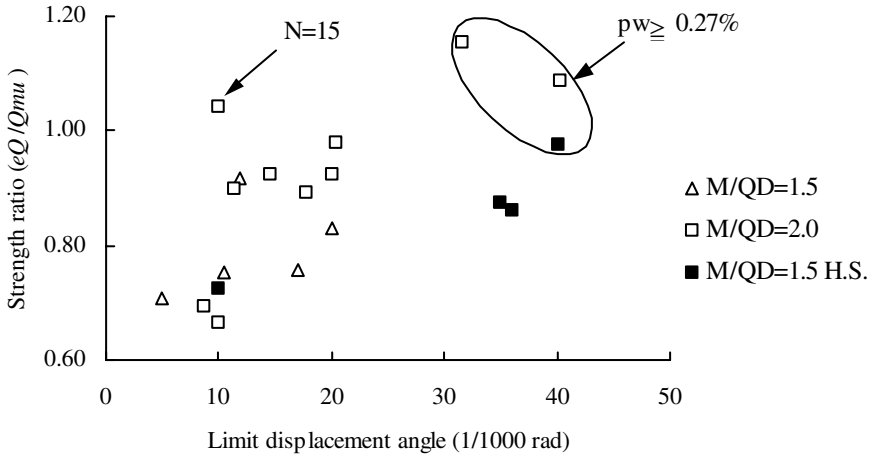

Fig. 10 Strength ratio-Limit displacement ralationship

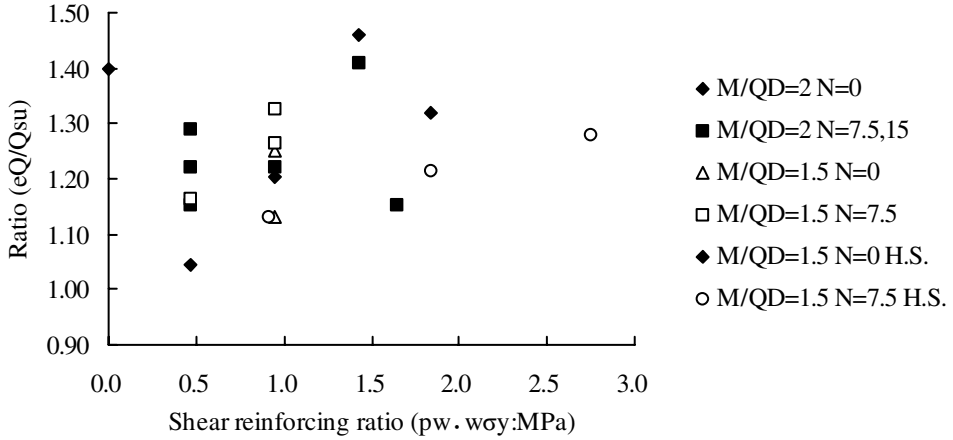

Fig.11 Comparison of calculated and experimental shear strength

Table 5 Comparispn with calculation

Specimen	Shear-span ratio *M*/*QD*	Lateral reinforce *pw* (%)	Axial stress *N* (MPa)	Maximum strength e*Q* (KN)	Ohno-Arakawa		A method		B method	
					Qsu (KN)	*eQ*/*Qsu*	*Qa* (KN)	*eQ*/*Qa*	*Qb* (KN)	*eQ*/*Qb*
No.1	1.50	0.095	7.5	200	172	1.16	93.7	2.13	139	1.44
No.2	〃	0.189	0	172	152	1.13	132	1.30	148	1.16
No.3	〃	〃	〃	180	144	1.25	125	1.44	132	1.36
No.4	〃	〃	7.5	256	193	1.33	132	1.94	184	1.39
No.5	〃	〃	〃	234	185	1.26	125	1.87	158	1.48
No.6	2.00	0	0	114	81.0	1.41	76	1.50	75	1.52
No.7	〃	0.095	0	119	114	1.04	101	1.18	100	1.19
No.8	〃	〃	7.5	188	154	1.22	101	1.86	128	1.47
No.9	〃	〃	〃	196	170	1.15	136	1.44	147	1.33
No.10	〃	〃	15	225	195	1.15	101	2.23	128	1.76
No.11	〃	〃	-2.5,7.5	192	149	1.29	82.7	2.32	111	1.73
No.12	〃	0.189	0	153	127	1.20	132	1.16	126	1.21
No.13	〃	〃	7.5	205	168	1.22	132	1.55	154	1.33
No.14	〃	0.287	0	194	133	1.46	120	1.62	131	1.48
No.15	〃	〃	7.5	245	174	1.41	156	1.57	151	1.62
No.16	1.50	0.092	7.5	344	304	1.13	220	1.56	278	1.24
No.17	〃	0.185	0	350	265	1.32	313	1.12	306	1.14
No.18	〃	〃	7.5	409	337	1.21	313	1.31	347	1.18
No.19	〃	0.277	〃	464	363	1.28	354	1.31	416	1.12
Average						1.24		1.60		1.38

CONCLUSIONS

The results of experiments are summarized as follows.

1. The shear strengths calculated from the Ohno-Arakawa equations are relatively in good agreement with the experimental results. The average shear strength ratio of the specimens to the calculated strengths was about 1.2.
2. Minimum shear reinforcing ratios to prevent sudden collapse in shear was necessary. The specimens exceeded the flexural yield strength showed relatively stable behavior until their failure in spite of rapid decrease in rigidity.
3. The deformational characteristics varied with the shear reinforcing ratios. The specimens exceeded the full flexural strength showed enough performance in displacement.
4. The shear strength became higher considerably when the axial load was applied to the specimens. It is necessary to consider the effect of axial stress in equations for estimating the shear strength of concrete piles.

REFERENCES

1. Yamakata, K., “Damage of building pile foundations in South Hyogo prefecture earthquake and its future measures,” J. of Soil and Foundations, Vol.24, No.11, pp.9-16, 1996.
2. Yamamoto, T., et al., “Experimental study on strength evaluation of cast-in-place concrete piles and their connections Part 5,” Proceedings of AIJ, pp.719-720, 1998.

3. Sakou, S., Yamada, K. and Yamamoto, T., "Fundamental study of reinforced concrete piles on shear behavior," Proceedings of JCI, Vol.21, No.3, pp.493-498, 1999.
4. Yoshida, M., Yamada, K. and Yamamoto, T., "An experimental study of reinforced concrete piles on shear-flexural behavior," Proceedings of JCI, Vol.21, No.3, pp.487-492, 1999.
5. Muto, K., "Inelastic Analysis of Reinforced Concrete Structures," Vol.2, pp.41-70, Maruzen, Tokyo, 1964.
6. AIJ, "Standard for Structural Calculation of Reinforced Concrete Structures," Architectural Institute of Japan, pp.136-153, 1999.
7. AIJ, "Design Guidelines for Earthquake Resistant Reinforced Concrete Buildings Based on Inelastic Displacement Concept (Draft)," Architectural Institute of Japan, 1997, 440 pp.